Received February 23, 2018, accepted April 23, 2018, date of publication April 30, 2018, date of current version May 24, 2018.

Digital Object Identifier 10.1109/ACCESS.2018.2831664

Cognitive Full-Duplex Decode-and-Forward Relaying Networks With Usable Direct Link and Transmit-Power Constraints

EDGAR EDUARDO BENITEZ OLIVO[1], (Member, IEEE), DIANA PAMELA MOYA OSORIO[2], (Member, IEEE), HIRLEY ALVES[3], (Member, IEEE), JOSÉ CÂNDIDO SILVEIRA SANTOS FILHO[4], (Member, IEEE), AND MATTI LATVA-AHO[3], (Senior Member, IEEE)

[1]São Paulo State University (UNESP), Campus of São João da Boa Vista, 13876-750 São João da Boa Vista, Brazil
[2]Center of Exact Sciences and Technology, Department of Electrical Engineering, Federal University of São Carlos, 13565-905 São Carlos, Brazil
[3]Centre for Wireless Communications, University of Oulu, 90014 Oulu, Finland
[4]Department of Communications, School of Electrical and Computer Engineering, University of Campinas, 13083-852 Campinas, Brazil

Corresponding author: Edgar Eduardo Benitez Olivo (edgar.olivo@unesp.br)

This work was supported by the Academy of Finland through the Project SAFE under Grant 303532.

ABSTRACT The performance of an underlay cognitive radio network that coexists with a primary destination is studied in terms of the outage probability. The investigated secondary network comprises a source-destination pair communicating under the assistance of a full-duplex decode-and-forward relay. We consider the following key aspects pertinent to the underlay cognitive-radio approach and to the full-duplex operation at the relay: the transmit power constraint of the cognitive network by the *maximum interference tolerated* at the primary destination, as well as by the *maximum-available transmit power* at the cognitive terminals; the impact of the residual self-interference inherent to the relay; and the use of a joint-decoding technique at the destination in order to combine the concurrent signals coming from the source and relay, which enables the treatment of the direct-link transmission as information signal, rather than as interference. Herein, the joint effect of the maximum interference power constraint and the residual self-interference are both examined. To this end, an *arbitrary power allocation* between source and relay is allowed. Then, an accurate closed-form approximation to the outage probability is proposed, from which an asymptotic expression is derived for the high SNR ratio regime. Our analytical results are validated via Monte Carlo simulations. Importantly, we show that a maximum-available transmit power not only saves energy but also reduces the outage probability at medium to high SNR ratio.

INDEX TERMS Cooperative diversity, decode-and-forward, full-duplex relaying, outage probability, underlay spectrum sharing.

I. INTRODUCTION

In recent years, wireless networks have become ubiquitous and an indispensable part of our daily lives due to a broad range of applications. We experience this through a myriad of connected devices that are changing the way we live, do business, gather into social groups, and interact in an ever more connected society. As a result of this high demand for wireless data services, a thousand-fold increase in traffic volume is expected by 2020 [1], [2]. Therefore, operators are compelled to cope with such demand and explore new ways to improve coverage, network capacity, and reliability, while lowering their capital and operating expenditures. Nonetheless, current technologies are unable to handle such stringent requirements; thus, new technologies, as well as new policies and a rearrangement of the spectrum usage, are required [3].

Spectrum sharing and full-duplex (FD) relaying appear as key technologies to boost coverage, energy efficiency, and spectral efficiency in order to cope with such galloping demand for mobile traffic in future wireless networks [4], [5]. Spectrum sharing was envisaged as a way to make a more efficient use of the radio spectrum, thus alleviating the spectrum scarcity and underutilization problems [6]. In particular, spectrum-sharing techniques enable secondary (unlicensed) users to exploit the cognition of their surroundings to access the licensed radio spectrum, provided that the primary users' performance is not compromised, by totally avoiding or limiting the resulting interference. According to the

spectrum-sharing approach, a cognitive radio transmission can be classified as underlay, overlay, or interweave [7], [8]. In this work, we focus on the performance analysis of secondary networks operating according to an underlay spectrum-sharing approach, whereby the secondary users are allowed to concurrently access the licensed band, provided that the resulting interference power on the primary users remains below a certain tolerated level, referred to as interference-temperature constraint [9].

In parallel to spectrum-sharing techniques, cooperative relaying re-emerged in early 2000s as a viable solution to improve energy efficiency and reliability, by providing a new form of spatial diversity to the communication process among single-antenna devices [10], [11]. However, most of the research in the field has focused on half-duplex (HD) relaying schemes [12], which are intrinsically inefficient in terms of spectrum usage, as the communication process occurs in orthogonal time slots, thereby expending at least twice the channel resources needed by a direct-link transmission. In light of this, full-duplex (FD) communications have gained an increasing attention from academia and industry in recent years, since FD nodes are able to support transmission and reception of signals under the same time and frequency resources (i.e., the so-called *in-band* FD communication) [5]. However, such a spectral-efficiency gain comes at the cost of some self-interference caused by the transmit signal on the receive signal at the same node, which can severely impair the communication performance [13]. Several research groups have addressed this issue by proposing self-interference cancellation techniques and new transceiver designs, as well as by implementing advanced FD prototypes, which have been shown to significantly mitigate the self-interference. However, the mitigation levels reported in those studies do not yet allow the interference to be neglected or considered as noise [13]–[17]. As a consequence, FD nodes suffer from some level of residual self-interference (RSI). All in all, those latter accomplishments indicate the feasibility of FD communication and its applicability in future wireless networks, as shall be further discussed in Section IV. In fact, the advances on the FD transceiver design have rendered FD relaying a promising solution to boost spectral efficiency in cooperative relaying networks, since a FD relay—unlike its HD-based counterpart—is able to simultaneously receive and forward data on the same carrier frequency [17]–[19], [21]–[23].

On the other hand, one important aspect regarding the analysis of cooperative relaying networks is that the direct link between source and destination is usually overlooked—or treated as a source of interference in the particular case of FD relaying (see, e.g., [17], [18])—so that most works focus on dual-hop (or multi-hop) relaying strategies. Nonetheless, the diversity order and spectral efficiency of both full- and half-duplex relaying can be improved when the direct-link transmission is seen and treated as useful information [19], [21]–[24]. Specifically, in FD relaying networks operating under the decode-and-forward (DF) protocol, coding schemes that enable the destination to handle simultaneously the source and relay information signals, which are referred to herein as joint-decoding (JD) schemes, can be achieved through either regular encoding with sliding-window decoding [25] or regular encoding with backward decoding [26].[1] An extension of those schemes to more general scenarios was performed in [27], and some applications to FD relaying schemes have been investigated in [19]–[22].

A. RELATED WORK

The combination of the aforementioned techniques—underlay spectrum sharing and FD relaying—in cognitive relaying networks (CRNs) has arisen as an appealing solution to cope with the demand of upcoming wireless networks, since both the overall system spectral efficiency and the secondary-network performance can be improved. In this context, several works have analyzed the performance of underlay CRNs, but most studies have focused on HD relaying schemes. Studies on FD relaying in a spectrum-sharing context are still incipient (see, e.g., [28]–[32], [35]). In [28], the idea of a secondary FD-DF relaying network with underlay spectrum sharing was first introduced. In that work, a scheme that considers equal power allocation (EPA) between the secondary source and relay was proposed, in which the transmit power of the secondary terminals is constrained by the maximum interference power tolerated at the primary network. Therein, the secondary network was considered to be impaired by two sources of interference: (i) the residual self-interference at the FD relay, and (ii) the transmission from the source via the direct link at the destination, as it takes place simultaneously with the transmission from the FD relay. Very recently, such analysis was extended in [29], by exploiting the transmission from the source via the direct link as an information signal (rather than as interference) and performing JD at the destination. On the other hand, in [30] and [31], an outage analysis was performed for opportunistic FD-DF relay selection. In those analyses, the self-interference at the secondary relays was taken into account; however, in [30] the direct-link transmission was treated as interference at the secondary destination, while in [31] the direct-link transmission was ignored altogether. Despite these valuable contributions, a critical aspect regarding the systems studied in [28]–[31] is that the maximum allowed transmit power at the secondary terminals was assumed unlimited, since the transmit power was defined as the ratio between the maximum interference power constraint and the channel power gain from the secondary terminal to the primary destination.

Besides the above-mentioned works, in [32], three relay selection criteria were analyzed in terms of the outage performance, for the FD amplify-and-forward relaying protocol and underlay spectrum-sharing constraints (i.e, the interference temperature constraint at the primary receiver and the

[1] Please refer to Section II-A for more details.

maximum transmit-power constraint at secondary terminals). That work was later extended in [33], in which the lower bounds of the outage probability for the system considered in [32] were determined. Nevertheless, in those studies, the effect of the direct-link transmission on the outage performance was disregarded, and equal power allocation between the secondary source and relay was assumed.

In [34], the performance in terms of the outage probability and capacity for the secondary users in an underlay cognitive network with opportunistic relay selection was studied, considering two-way FD-based relays. In that case, the presence of the direct link and the maximum transmit power limit at secondary terminals were not considered. In [35], we presented an adaptive transmission scheme for a cognitive DF relaying network, whereby one out of the following transmission modes is selected based on the channel conditions: HD relaying, FD relaying, or direct-link transmission.

Additionally, in the context of physical layer security, the secrecy outage probability for three relay selection schemes was studied in [36], for a full-duplex heterogeneous network in the presence of multiple cognitive radio eavesdroppers.

More recently, in [37], the outage performance of optimal and partial relay selection schemes was analyzed for a cognitive relaying network with full-duplex decode-and-forward relays, under the presence of multiple primary receivers. Therein, the transmission between the secondary source and destination is performed in two hops, thus neglecting the existence of the direct link. In addition, the transmit power at secondary nodes depends only on the interference temperature of the primary network, thus the effect of the maximum-available transmit power on the outage performance is not considered. In [38], a power allocation policy between the secondary source and relay, based on average channel state information (CSI), is proposed for a full-duplex amplify-and-forward cognitive relaying network, in order to optimize the capacity. In that work, the direct-link transmission is also disregarded.

B. SUMMARY OF CONTRIBUTIONS

In contrast to the schemes in [28] and [30], but similarly to the scheme in [29], herein we shall exploit the transmission through the direct link as an useful information signal, rather than as interference, by assuming a JD reception at the destination. In addition, differently from [28]–[31], the total transmit power at the secondary terminals is considered to be limited by not only a maximum interference power tolerated at the primary destination, but also a maximum-available transmit power at the secondary terminals. In this context, we derive an accurate closed-form approximation to the exact outage probability for a three-terminal cognitive FD-DF relaying network that employs JD reception at the secondary destination, under spectrum-sharing constraints, by means of which the combined effect of both the maximum interference power tolerated at the primary destination and the RSI at the secondary relay is investigated. It is worthwhile to mention that although the work in [35] addresses a hybrid scheme which includes the FD-relaying transmission mode, the performance of the fixed FD relaying scheme presented herein cannot be derived or assessed as a particular case of the analytical results obtained in [35]. The proposals of the referred schemes are different, thus requiring separate analyses. The following are our main contributions:

- We extend the results from [28] and [29] by accounting for the maximum-available transmit power at the secondary source and relay.
- For the proposed setup, we derive exact closed-form expressions for the cumulative distribution function (CDF) of the instantaneous received signal-to-interference-plus-noise ratio (SINR) at the secondary relay and the instantaneous received signal-to-noise ratio (SNR) at the secondary destination are also provided.
- We propose a closed-form approximation to the outage probability of the considered scheme, in which the transmission from the source through the direct link is processed as an information signal, rather than as interference.
- We call attention to the fact that the instantaneous received SNRs of the first hop and direct link, and those of the second hop and self-interference link, are correlated random variables (RVs). It is worth mentioning that this correlation, concerning the analysis of cognitive FD relaying networks, has been overlooked in the literature (see, e.g., [28], [29], [32]). In particular, the analyses in [28], [29], and [32] were presented as exact solutions for the outage probability, but those analyses were performed by assuming statistical independence between the referred RVs, thereby being approximate solutions, indeed. In spite of that, such an assumption turned out to render tight approximations to the exact outage probabilities of the systems considered in those works, as can be observed from the sample examples therein. We have empirically verified that the same holds true in our case. So we shall adopt the referred independence as an approximate analytical framework.
- A closed-form asymptotic analysis is presented for the outage performance, whereby the outage floor at high SNR is characterized, as well as the effect of the maximum interference level tolerated at the primary destination is assessed.
- We investigate the impact of different power allocations between source and relay at the cognitive network.
- An extensive set of numerical results is provided, which compares the performance of the proposed scheme to those of the schemes presented in [28] and [29]. Our results show that a maximum-available transmit power not only saves energy but also reduces the outage probability at medium to high SNR.

An outline of the paper is as follows. In Section II, the system model for cognitive FD-DF relaying networks with usable

direct link is characterized. In Section III, a highly accurate approximation to the exact outage probability of the scheme under investigation is presented in closed form. In addition, an asymptotic outage analysis is carried out to describe its behavior at high SNR. Section IV shows numerical results that validate the foregoing analysis. Finally, the main conclusions are drawn in Section V.

Notation: Throughout this paper, $f_X(\cdot)$ and $F_X(\cdot)$ represent the probability density function (PDF) and CDF of a RV X, respectively, $E[\cdot]$ is the expectation operator, and $\Pr[\cdot]$ stands for probability.

II. SYSTEM MODEL

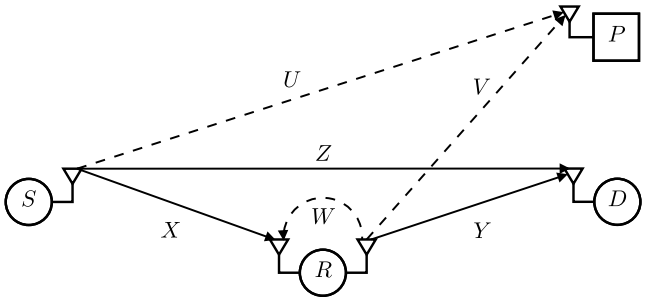

FIGURE 1. System model of an underlay cognitive relaying network consisting of one source (*S*), one FD relay (*R*), and one destination (*D*), which operates in the licensed spectrum owned by a primary destination (*P*). The data links are represent by solid lines, while the interference links are represented by dashed lines. Note that *R* suffers from self-interference.

As illustrated in Fig. 1, the considered underlay cognitive relaying network consists of one source terminal (S), one FD-DF relay terminal (R), and one destination terminal (D), which operate subject to the power constraints inflicted by a primary destination (P). We summarize the system-model assumptions as follows:

(i) All terminals are supposed to be equipped with a single antenna, except for the secondary relay, which is equipped with one pair of transmit and receive antennas. Indeed, by employing a two-antenna setup, a high physical isolation between the antennas at the FD relay can be achieved, in order to alleviate the self-interference [18].

(ii) The channel coefficients of the data links $S \to R$, $R \to D$, and $S \to D$ are denoted by h_X, h_Y, and h_Z, respectively; the channel coefficient of the RSI link at R is denoted by h_W; and the channel coefficients of the interference links $S \to P$ and $R \to P$ are denoted by h_U and h_V, respectively.

(iii) All wireless links, including that of the RSI, exhibit independent and non-identically distributed (i.n.i.d.) block Rayleigh fading. Thus, the corresponding channel power gains $g_A = |h_A|^2$, $A \in \{U, V, W, X, Y, Z\}$, are exponentially distributed with average value $\Omega_A = E[|h_A|^2]$, while the channel coefficients are supposed to remain constant during each data transfer block, but change independently over consecutive blocks. It is noteworthy that, as a common assumption in FD relaying (see, for example, [18], [19], [21]–[23], [28]–[32]), the RSI link at R is also modeled as a Rayleigh fading channel, by considering that the scattering component prevails over the specular component, once this latter is significantly attenuated upon using passive and active self-interference mitigation techniques [13]–[17].

(iv) The maximum interference power tolerated at P, coming from the cognitive network, is denoted by I.

Bearing the above assumptions in mind, the transmit powers at the secondary source and relay, P_S and P_R, are constrained as

$$g_U P_S + g_V P_R \leq I, \tag{1}$$

where

$$P_S = \min\left\{\frac{\eta I}{g_U}, P_{\mathrm{T}}\right\} = \begin{cases} P_{\mathrm{T}} & \text{if } g_U \leq \eta I/P_{\mathrm{T}} \\ \eta I/g_U & \text{otherwise,} \end{cases} \tag{2}$$

$$P_R = \min\left\{\frac{\bar{\eta} I}{g_V}, P_{\mathrm{T}}\right\} = \begin{cases} P_{\mathrm{T}} & \text{if } g_V \leq \bar{\eta} I/P_{\mathrm{T}} \\ \bar{\eta} I/g_V & \text{otherwise,} \end{cases} \tag{3}$$

with P_{T} being the maximum-available transmit power at S and R, $0 \leq \eta \leq 1$ being an arbitrary power allocation factor between S and R, and $\bar{\eta} = 1 - \eta$, in order to satisfy the constraint in (1).

Then, the instantaneous received SNRs of the data links $S \to R$, $R \to D$, $S \to D$, and that of the self-interference link can be expressed as $X = g_X P_S/N_0$, $Y = g_Y P_R/N_0$, $Z = g_Z P_S/N_0$, and $W = g_W P_R/N_0$, respectively, where P_S and P_R are given by (2) and (3), and N_0 is the mean power of the background noise at all secondary nodes, which is assumed to be AWGN. Now, by defining $\bar{\gamma}_P \triangleq P_{\mathrm{T}}/N_0$ as the maximum transmit SNR at the secondary terminals and $\bar{\gamma}_I \triangleq I/N_0$ as the maximum interference-to-noise ratio tolerated at the primary destination, we have that X, Y, Z, and W can be written, respectively, as

$$X = \min\left\{\frac{\eta\bar{\gamma}_I}{g_U}, \bar{\gamma}_P\right\} g_X, \tag{4a}$$

$$Y = \min\left\{\frac{\bar{\eta}\bar{\gamma}_I}{g_V}, \bar{\gamma}_P\right\} g_Y, \tag{4b}$$

$$Z = \min\left\{\frac{\eta\bar{\gamma}_I}{g_U}, \bar{\gamma}_P\right\} g_Z, \tag{4c}$$

$$W = \min\left\{\frac{\bar{\eta}\bar{\gamma}_I}{g_V}, \bar{\gamma}_P\right\} g_W. \tag{4d}$$

Then, the instantaneous received SINR at the secondary relay, γ_R, and the instantaneous received SNR at the secondary destination, γ_D, are obtained, respectively, as

$$\begin{aligned} \gamma_R &= \frac{g_X P_S}{N_0 + g_W P_R} \\ &= \frac{g_X \frac{P_S}{N_0}}{1 + g_W \frac{P_R}{N_0}} \\ &= \frac{X}{1 + W}, \end{aligned} \tag{5}$$

$$\begin{aligned}\gamma_D &= \frac{g_Y P_R + g_Z P_S}{N_0} \\ &= g_Y \frac{P_R}{N_0} + g_Z \frac{P_S}{N_0} \\ &= Y + Z. \end{aligned} \tag{6}$$

Note in (6) that the secondary destination treats the transmission coming from the direct link as an information signal, in contrast to the schemes in [28, eqs. (13) and (18)], where this transmission is treated as an interference signal. This is enabled by using a JD technique, as described next.

A. JOINT-DECODING SCHEME

As in [19], [20], [29], and [30], herein the direct-link transmission is assumed to be exploited as a source of information through a JD technique. As discussed in those works, such a technique relies on a combination of block-Markov encoding at the source and relay, associated with coding for the cooperative multiple access channel and superposition coding [27], [39], which is referred to as irregular encoding/successive decoding [27]. As remarked in [27], the same target rates can be achieved through different strategies, such as regular encoding/sliding-window decoding [25] and regular encoding/backward decoding [26].

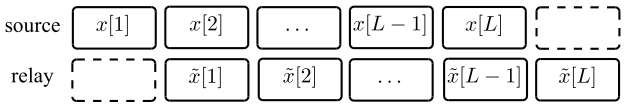

FIGURE 2. Joint decoding. The message of the source is split into L blocks. Note that the message of the relay is one block delayed compared to that of the source. After receiving the last block from the relay, the destination applies backward decoding to jointly decode the messages from both source and relay.

For illustration, let us consider a regular encoding/backward decoding scheme, as depicted in Fig. 2. As proposed in [26] and revisited in [20] and [29], we observe from Fig. 2 that the source message x is split into L blocks. In addition, the re-encoded message at the relay, $\tilde{x}$, is delayed with respect to x, such that $\tilde{x}[l] = x[l - T_d]$, where $1 \leq l \leq L$ and T_d stands for a processing delay. For simplicity, we assume $T_d = 1$, which means that the relay message is delayed only by one block with respect to the source message. However, it is worthwhile to mention that the performance of regular encoding/backward decoding is not affected for large L, as long as the ratio between the delay and number of blocks, T_d/L, is small [21]. At the destination, after receiving the last block from the relay, a backward decoding technique is applied to jointly decode the messages.

For such a joint-decoding technique, it is shown in [29] that the instantaneous received SNR at the destination can be obtained via maximal-ratio combining as in (6).

III. OUTAGE PROBABILITY

In this section, approximate and asymptotic analytical expressions for the outage probability of the considered scheme are introduced by Theorems 1, 2, and 3 in closed form. For the asymptotic analysis, we consider the following two cases: (*i*) P_{T} varying independently of I (that is, considering a fixed value of the interference temperature), and (*ii*) P_{T} varying proportionally to I. First, let us define the corresponding outage event.

Definition 1: For the proposed setup, the secondary network is in outage if the instantaneous end-to-end SNR is less than a given threshold τ. Thus, for the DF relaying protocol, the outage probability can be written as [19]–[21]

$$\begin{aligned} P_{\mathrm{out}} &= \Pr\left[\min\left\{\gamma_R, \gamma_D\right\} < \tau\right] \\ &= \Pr\left[\gamma_R < \tau\right] + \Pr\left[\gamma_D < \tau\right] - \Pr\left[\gamma_R < \tau, \gamma_D < \tau\right] \\ &= F_{\gamma_R}(\tau) + F_{\gamma_D}(\tau) - F_{\gamma_R,\gamma_D}(\tau, \tau), \end{aligned} \tag{7}$$

where the instantaneous received SINR at the secondary relay and the instantaneous received SNR at the secondary destination, γ_R and γ_D, are given by (5) and (6), respectively.

Remark 1: Note from (5) and (6) and from the definitions of X, Y, Z, and W in (4) that γ_R and γ_D are correlated RVs, although this has been overlooked in previous works [28], [29], [32]. More specifically, both instantaneous received SNRs X and Z depend on the channel power gain g_U, which corresponds to the interference link $S \rightarrow P$. Similarly, both instantaneous received SNRs W and Y depend on the channel power gain g_V, which corresponds to the interference link $R \rightarrow P$. Hence, the joint CDF in (7) is not given by the product of the marginal CDFs, i.e., $F_{\gamma_R,\gamma_D}(\cdot,\cdot) \neq F_{\gamma_R}(\cdot)F_{\gamma_D}(\cdot)$, as often assumed in previous works [28], [29], [32]. But finding this joint CDF is a rather difficult task, which renders approximate solutions especially attractive. In particular, as in [28], [29], and [32], γ_R and γ_D can be assumed to be independent. Next we assume this to allow for an approximate solution. More importantly, we show that the resulting approximation is highly accurate over the whole range of transmit SNR values, irrespective of the average RSI channel power at the secondary relay and the interference power constraint at the primary destination.

Now we state Lemma 1, which will be helpful for proving Theorem 1.

Lemma 1: The CDF and PDF for the instantaneous received SNR X at the first hop are given by

$$F_X(x) = 1 - e^{-\frac{x}{\bar{\gamma}_P \Omega_X}} \left(1 - \frac{x\Omega_U e^{-\frac{\eta\bar{\gamma}_I}{\bar{\gamma}_P \Omega_U}}}{\eta\bar{\gamma}_I\Omega_X + x\Omega_U}\right), \tag{8}$$

$$\begin{aligned} f_X(x) = {} & \frac{e^{-\frac{x}{\bar{\gamma}_P\Omega_X}}}{\bar{\gamma}_P\Omega_X} \\ & \times\left[1 - \frac{\Omega_U e^{-\frac{\eta\bar{\gamma}_I}{\bar{\gamma}_P\Omega_U}}\left(x^2\Omega_U + x\eta\bar{\gamma}_I\Omega_X - \eta\bar{\gamma}_I\bar{\gamma}_P\Omega_X^2\right)}{(\eta\bar{\gamma}_I\Omega_X + x\Omega_U)^2}\right]. \end{aligned} \tag{9}$$

Proof: Please refer to Appendix A. ■

Following the same rationale, the CDFs and PDFs for Z, W, and Y can be shown to be attained as in (8) and (9), with the following substitutions: Ω_X by Ω_Z, for Z; Ω_X, Ω_U, and

η by Ω_W, Ω_V, and $\bar{\eta}$, for W; and Ω_X, Ω_U, and η by Ω_Y, Ω_V, and $\bar{\eta}$, for Y.

Next we introduce two theorems concerning the outage performance of the proposed scheme.

Theorem 1: In a secondary network with spectrum-sharing constraints, FD-DF transmission at the relay, and JD reception at the destination, an accurate approximation to the outage probability is given in closed form as

$$P_{\text{out}} \approx F_{\gamma_R}(\tau) + F_{\gamma_D}(\tau) - F_{\gamma_R}(\tau) F_{\gamma_D}(\tau), \tag{10}$$

where τ is the target SNR threshold, and γ_R and γ_D are respectively the instantaneous received SINR at the secondary relay and the instantaneous received SNR at the secondary destination, given by (5) and (6), the CDFs of which are computed as in (11) and (12), shown in the next page. In those expressions, Ei $(\cdot)$ stands for the exponential integral function [40, eq. (8.211.1)].

Proof: Please refer to Appendix B. ∎

In the following theorem, an asymptotic expression in the high-SNR regime for the approximation given in (10), considering that P_{T} varies independently of I, is presented in closed form.

Theorem 2: In a secondary network with spectrum-sharing constraints, FD-DF transmission at the relay, and JD reception at the destination, the asymptotic outage performance at high SNR is determined as

$$\begin{aligned} P_{\text{out}} \simeq\ & \frac{\Omega_U \tau\left(\Omega_V - \bar{\eta}\bar{\gamma}_I \Omega_W\right)}{\Omega_U \tau\left(\Omega_V - \bar{\eta}\bar{\gamma}_I \Omega_W\right) + \eta\bar{\gamma}_I \Omega_X \Omega_V} \\ & + \frac{\eta\bar{\eta}\bar{\gamma}_I^2 \Omega_X \Omega_W \Omega_U \Omega_V \tau}{\left[\Omega_U \tau\left(\Omega_V - \bar{\eta}\bar{\gamma}_I \Omega_W\right) + \eta\bar{\gamma}_I \Omega_X \Omega_V\right]^2} \\ & \times \log\left(\frac{\Omega_U \Omega_V \tau + \eta\bar{\gamma}_I \Omega_X \Omega_V}{\bar{\eta}\bar{\gamma}_I \Omega_W \Omega_U \tau}\right). \end{aligned} \tag{13}$$

Proof: By considering that the maximum-available transmit power at the secondary terminals, P_{T}, varies independently of the maximum interference power tolerated at the primary destination, I, it follows that all the terms proportional to $1/\bar{\gamma}_P$ tend to zero as P_{T} increases in the high-SNR regime (see the definition for $\bar{\gamma}_P$ in Section II). Additionally, using the Maclaurin expression for the exponential function [40, eq. (0.318.2)], we have that $e^{-\lambda} \simeq 1 - \lambda$ for small λ. Applying this into (10) with use of (11) and (12), and disregarding the high-order terms in respect to $1/\bar{\gamma}_P$, by some algebraic manipulations, an asymptotic expression for the outage probability can be obtained in closed form as in (13). ∎

Remark 2: Note from (13) that the asymptotic outage probability is independent of $\bar{\gamma}_P$, thereby resulting in a floor, expressed in terms of the following system parameters: the average channel powers of the data link $S \to D$ (Ω_X), the self-interference link (Ω_W), and the interference links $S \to P$ (Ω_U) and $R \to P$ (Ω_V); the power allocation factor η; and the maximum interference-to-noise ratio tolerated at the primary destination $(\bar{\gamma}_I)$. Hence, the diversity order [41] for the considered system becomes zero. In the next section, numerical results illustrate how the referred system parameters affect the asymptotic outage performance.

Now, by considering that P_{T} varies proportionally to I, an asymptotic expression at high SNR for the approximation given in (10) is obtained in closed form as follows.

Theorem 3: The asymptotic outage probability for a secondary network with spectrum-sharing constraints, FD-DF transmission at the relay, and JD reception at the destination, in which the maximum-available transmit power at the secondary terminals is varied proportionally to the interference power constraint at the primary destination, is obtained as

$$\begin{aligned} & P_{\text{out}} \\ & \simeq 1 - \frac{\Omega_X\left(1 - e^{-\frac{\eta}{\Omega_U}}\right)\left(1 - e^{-\frac{\bar{\eta}}{\Omega_V}}\right)}{\tau\Omega_W + \Omega_X} \\ & \quad - \frac{\eta\Omega_X\left(e^{\bar{\eta}/\Omega_V} - 1\right) e^{-\frac{\eta}{\Omega_U} - \frac{\bar{\eta}}{\Omega_V}} \log\left(1 + \frac{\tau\Omega_U\Omega_W}{\eta\tau\Omega_W + \eta\Omega_X}\right)}{\tau\Omega_U\Omega_W} \\ & \quad - \frac{\left(e^{\eta/\Omega_U} - 1\right) e^{-\frac{\eta}{\Omega_U} - \frac{\bar{\eta}}{\Omega_V}}}{\Omega_V\Omega_X} \\ & \quad \times \left(\Omega_V\Omega_X - \bar{\eta}\tau\Omega_W \log\left(1 + \frac{\Omega_V\Omega_X}{\bar{\eta}\tau\Omega_W + \bar{\eta}\Omega_X}\right)\right) \\ & \quad + \frac{\eta e^{-\frac{\eta}{\Omega_U} - \frac{\bar{\eta}}{\Omega_V}}}{(\bar{\eta}\tau\Omega_U\Omega_W - \eta\Omega_V\Omega_X)^2}\Big\{\Omega_V\Omega_X(\bar{\eta}\tau\Omega_U\Omega_W - \eta\Omega_V\Omega_X) \\ & \quad + \bar{\eta}\Omega_X\left[\eta\Omega_V\Omega_X - \tau\Omega_U\Omega_W(\bar{\eta} + \Omega_V)\right] \\ & \quad \times \log\left(1 + \frac{\tau\Omega_U\Omega_W}{\eta\tau\Omega_W + \eta\Omega_X}\right) \\ & \quad + \bar{\eta}\tau\Omega_W\left[\Omega_V\Omega_X(\eta + \Omega_U) - \bar{\eta}\tau\Omega_U\Omega_W\right] \\ & \quad \times \log\left(1 + \frac{\Omega_V\Omega_X}{\bar{\eta}\tau\Omega_W + \bar{\eta}\Omega_X}\right)\Big\}. \end{aligned} \tag{14}$$

Proof: The proof follows a rationale similar to that of Theorem 2, but in this case, since $P_{\text{T}} \propto I$, we have that all the terms proportional to $1/\bar{\gamma}_P$ and, consequently, those terms proportional to $1/\bar{\gamma}_I$, go to zero as P_{T} becomes larger in the high-SNR regime. Therefore, from (10), by using (11) and (12), neglecting the high-order terms with respect to $1/\bar{\gamma}_P$ and $1/\bar{\gamma}_I$, and after some simplifications, an asymptotic closed-form expression for the outage probability can be attained as in (14). ∎

Remark 3: Note from (14) that, for $P_{\text{T}} \propto I$, the asymptotic outage performance is expressed in terms of the same system parameters as in (13) (in which a fixed value of the interference temperature I is considered), except that, in this case, the asymptotic outage performance is independent not only of $\bar{\gamma}_P$, but also of $\bar{\gamma}_I$. As a consequence, the diversity order of the system is also zero, which is expected because of the deleterious effect of RSI, inherent to FD relaying.

IV. NUMERICAL RESULTS AND DISCUSSIONS

In the following, the approximate and asymptotic outage expressions derived in Section III are evaluated through

$$
\begin{aligned}
&F_{\gamma_R}(\tau)\\
&= 1 - \frac{\bar{\gamma}_P\Omega_X e^{-\frac{\tau}{\bar{\gamma}_P\Omega_X}}}{\bar{\gamma}_P\Omega_W\tau + \bar{\gamma}_P\Omega_X}\left(1 - e^{-\frac{\eta\bar{\gamma}_I}{\bar{\gamma}_P\Omega_U}}\right)\left(1 - e^{-\frac{\bar{\eta}\bar{\gamma}_I}{\bar{\gamma}_P\Omega_V}}\right) - e^{-\left(\frac{\bar{\eta}\bar{\gamma}_I}{\bar{\gamma}_P\Omega_V} + \frac{\tau}{\bar{\gamma}_P\Omega_X}\right)}\left(1 - e^{-\frac{\eta\bar{\gamma}_I}{\bar{\gamma}_P\Omega_U}}\right)\\
&\times\left[1 + \frac{\bar{\eta}\bar{\gamma}_I\Omega_W\tau e^{\frac{\bar{\eta}\bar{\gamma}_I\Omega_W\tau + \bar{\eta}\bar{\gamma}_I\Omega_X}{\bar{\gamma}_P\Omega_X\Omega_V}}}{\bar{\gamma}_P\Omega_X\Omega_V}\mathrm{Ei}\left(-\frac{\bar{\eta}\bar{\gamma}_I\Omega_W\tau + \bar{\eta}\bar{\gamma}_I\Omega_X}{\bar{\gamma}_P\Omega_X\Omega_V}\right)\right] + \frac{\eta\bar{\gamma}_I\Omega_X e^{\frac{\Omega_U\tau + \eta\bar{\gamma}_I\Omega_X}{\bar{\gamma}_P\Omega_W\Omega_U\tau}}}{\bar{\gamma}_P\Omega_W\Omega_U\tau}\left(1 - e^{-\frac{\bar{\eta}\bar{\gamma}_I}{\bar{\gamma}_P\Omega_V}}\right)\\
&\times\mathrm{Ei}\left(-\frac{(\eta\bar{\gamma}_I\Omega_X + \Omega_U\tau)(\Omega_X + \Omega_W\tau)}{\bar{\gamma}_P\Omega_X\Omega_W\Omega_U\tau}\right) - \frac{e^{-\left(\frac{\bar{\eta}\bar{\gamma}_I}{\bar{\gamma}_P\Omega_V} + \frac{\eta\bar{\gamma}_I}{\bar{\gamma}_P\Omega_U} + \frac{\tau}{\bar{\gamma}_P\Omega_X}\right)}}{\left[\Omega_U\tau\left(\Omega_V - \bar{\eta}\bar{\gamma}_I\Omega_W\right) + \eta\bar{\gamma}_I\Omega_X\Omega_V\right]^2}\left\{\eta\bar{\gamma}_I\Omega_X\Omega_V\left[\Omega_U\tau\left(\Omega_V - \bar{\eta}\bar{\gamma}_I\Omega_W\right) + \eta\bar{\gamma}_I\Omega_X\Omega_V\right]\right.\\
&+ \bar{\eta}\bar{\gamma}_I\Omega_W\tau\left[\frac{\eta\bar{\gamma}_I\Omega_U\tau}{\bar{\gamma}_P}\left(\Omega_V - \bar{\eta}\bar{\gamma}_I\Omega_W\right) + \eta\bar{\gamma}_I\Omega_X\Omega_V\left(\Omega_U + \frac{\eta\bar{\gamma}_I}{\bar{\gamma}_P}\right)\right]\exp\left(\frac{\bar{\eta}\bar{\gamma}_I\Omega_X + \bar{\eta}\bar{\gamma}_I\Omega_W\tau}{\bar{\gamma}_P\Omega_X\Omega_V}\right)\mathrm{Ei}\left(-\frac{\bar{\eta}\bar{\gamma}_I\Omega_X + \bar{\eta}\bar{\gamma}_I\Omega_W\tau}{\bar{\gamma}_P\Omega_X\Omega_V}\right)\\
&-\left[\frac{\Omega_U\tau}{\bar{\gamma}_P}\left(\bar{\eta}\bar{\gamma}_I\bar{\gamma}_P\Omega_W\Omega_V - \bar{\eta}\bar{\gamma}_I\Omega_V + \bar{\eta}^2\bar{\gamma}_I^2\Omega_W\right) - \frac{\eta\bar{\eta}\bar{\gamma}_I^2\Omega_X\Omega_V}{\bar{\gamma}_P}\right]\eta\bar{\gamma}_I\Omega_X\exp\left(\frac{(\Omega_U\tau + \eta\bar{\gamma}_I\Omega_X)(\Omega_X + \Omega_W\tau)}{\bar{\gamma}_P\Omega_X\Omega_W\Omega_U\tau}\right)\\
&\left.\times\mathrm{Ei}\left(-\frac{(\eta\bar{\gamma}_I\Omega_X + \Omega_U\tau)(\Omega_X + \Omega_W\tau)}{\bar{\gamma}_P\Omega_X\Omega_W\Omega_U\tau}\right)\right\} \qquad (11)
\end{aligned}
$$

$$
\begin{aligned}
&F_{\gamma_D}(\tau)\\
&= 1 - \frac{\bar{\gamma}_P\Omega_Z}{\bar{\gamma}_P\Omega_Y - \bar{\gamma}_P\Omega_Z}\left(1 - e^{-\frac{\eta\bar{\gamma}_I}{\bar{\gamma}_P\Omega_U}}\right)\left(1 - e^{-\frac{\bar{\eta}\bar{\gamma}_I}{\bar{\gamma}_P\Omega_V}}\right)\left(e^{-\frac{\tau}{\bar{\gamma}_P\Omega_Y}} - e^{-\frac{\tau}{\bar{\gamma}_P\Omega_Z}}\right) - \frac{\bar{\eta}\bar{\gamma}_I\Omega_Y e^{-\frac{\bar{\eta}\bar{\gamma}_I}{\bar{\gamma}_P}\left(\frac{1}{\Omega_V} + \frac{\tau}{\bar{\eta}\bar{\gamma}_I\Omega_Y}\right)}}{\Omega_V\tau + \bar{\eta}\bar{\gamma}_I\Omega_Y}\\
&- e^{-\frac{\tau}{\bar{\gamma}_P\Omega_Y}}\left(1 - e^{-\frac{\bar{\eta}\bar{\gamma}_I}{\bar{\gamma}_P\Omega_V}}\right) + \frac{\eta\bar{\gamma}_I\Omega_Z\left(1 - e^{-\frac{\bar{\eta}\bar{\gamma}_I}{\bar{\gamma}_P\Omega_V}}\right)e^{-\frac{\Omega_U\tau + \eta\bar{\gamma}_I\Omega_Z}{\bar{\gamma}_P\Omega_Y\Omega_U}}}{\bar{\gamma}_P\Omega_Y\Omega_U}\left[\mathrm{Ei}\left(\frac{\eta\bar{\gamma}_I\Omega_Z - \eta\bar{\gamma}_I\Omega_Y}{\bar{\gamma}_P\Omega_Y\Omega_U}\right) - \mathrm{Ei}\left(\frac{(\Omega_Z - \Omega_Y)(\eta\bar{\gamma}_I\Omega_Z + \Omega_U\tau)}{\bar{\gamma}_P\Omega_Y\Omega_Z\Omega_U}\right)\right]\\
&- \frac{\left(1 - e^{-\frac{\eta\bar{\gamma}_I}{\bar{\gamma}_P\Omega_U}}\right)e^{-\frac{(\Omega_V\tau + \bar{\eta}\bar{\gamma}_I\Omega_Y)(\Omega_Y + \Omega_Z)}{\bar{\gamma}_P\Omega_Y\Omega_Z\Omega_V}}}{\Omega_V\bar{\gamma}_P\Omega_Z(\Omega_V\tau + \bar{\eta}\bar{\gamma}_I\Omega_Y)} \times\left\{\bar{\gamma}_P\Omega_Z\Omega_V e^{\frac{\bar{\eta}\bar{\gamma}_I\Omega_Y}{\bar{\gamma}_P\Omega_Z\Omega_V}}\left[\left(\Omega_V\tau + \bar{\eta}\bar{\gamma}_I\Omega_Y\right)e^{\frac{\tau}{\bar{\gamma}_P\Omega_Y}} - \bar{\eta}\bar{\gamma}_I\Omega_Y e^{\frac{\tau}{\bar{\gamma}_P\Omega_Z}}\right]\right.\\
&\left.- \bar{\eta}\bar{\gamma}_I\Omega_Y\left(\Omega_V\tau + \bar{\eta}\bar{\gamma}_I\Omega_Y\right)e^{\frac{\bar{\eta}\bar{\gamma}_I}{\bar{\gamma}_P}\left(\frac{1}{\Omega_V} + \frac{\tau}{\bar{\eta}\bar{\gamma}_I\Omega_Y}\right)}\left[\mathrm{Ei}\left(\frac{\bar{\eta}\bar{\gamma}_I\Omega_Y - \bar{\eta}\bar{\gamma}_I\Omega_Z}{\bar{\gamma}_P\Omega_Z\Omega_V}\right) - \mathrm{Ei}\left(\frac{(\Omega_Y - \Omega_Z)(\bar{\eta}\bar{\gamma}_I\Omega_Y + \Omega_V\tau)}{\bar{\gamma}_P\Omega_Y\Omega_Z\Omega_V}\right)\right]\right\}\\
&- \frac{\exp\left(-\frac{\Omega_V\Omega_U\tau\left(\Omega_Y + 2\Omega_Z\right) + \left(\eta\bar{\gamma}_I\Omega_Z\Omega_V + \bar{\eta}\bar{\gamma}_I\Omega_Y\Omega_U\right)\left(\Omega_Y + \Omega_Z\right)}{\bar{\gamma}_P\Omega_Y\Omega_Z\Omega_U\Omega_V}\right)}{\left(\Omega_V\tau + \bar{\eta}\bar{\gamma}_I\Omega_Y\right)\left[\Omega_U\left(\Omega_V\tau + \bar{\eta}\bar{\gamma}_I\Omega_Y\right) + \eta\bar{\gamma}_I\Omega_Z\Omega_V\right]^2}\\
&\times\left\{\Omega_V\eta\bar{\gamma}_I\Omega_Z\left[\Omega_U\left(\Omega_V\tau + \bar{\eta}\bar{\gamma}_I\Omega_Y\right) + \Omega_V\eta\bar{\gamma}_I\Omega_Z\right]\left[\left(\Omega_V\tau + \bar{\eta}\bar{\gamma}_I\Omega_Y\right)e^{\frac{\tau}{\bar{\gamma}_P\Omega_Y}} - \bar{\eta}\bar{\gamma}_I\Omega_Y e^{\frac{\tau}{\bar{\gamma}_P\Omega_Z}}\right]e^{\frac{\bar{\eta}\bar{\gamma}_I\Omega_Y}{\bar{\gamma}_P\Omega_Z\Omega_V} + \frac{\Omega_U\tau + \eta\bar{\gamma}_I\Omega_Z}{\bar{\gamma}_P\Omega_Y\Omega_U}}\right.\\
&+ \left(\Omega_V\tau + \bar{\eta}\bar{\gamma}_I\Omega_Y\right)\left\{-\bar{\eta}\bar{\gamma}_I\Omega_Y\left[\Omega_V\eta\bar{\gamma}_I\Omega_Z\left(\Omega_U + \frac{\eta\bar{\gamma}_I}{\bar{\gamma}_P}\right) + \frac{\eta\bar{\gamma}_I\Omega_U\Omega_V\tau}{\bar{\gamma}_P} + \frac{\eta\bar{\eta}\bar{\gamma}_I^2\Omega_Y\Omega_U}{\bar{\gamma}_P}\right]e^{\frac{\bar{\eta}\bar{\gamma}_I}{\bar{\gamma}_P}\left(\frac{1}{\Omega_V} + \frac{2\Omega_U\tau + \eta\bar{\gamma}_I\Omega_Z}{\bar{\eta}\bar{\gamma}_I\Omega_Y\Omega_U}\right)}\right.\\
&\times\left[\mathrm{Ei}\left(\frac{\bar{\eta}\bar{\gamma}_I\Omega_Y - \bar{\eta}\bar{\gamma}_I\Omega_Z}{\bar{\gamma}_P\Omega_Z\Omega_V}\right) - \mathrm{Ei}\left(\frac{(\Omega_Y - \Omega_Z)(\bar{\eta}\bar{\gamma}_I\Omega_Y + \Omega_V\tau)}{\bar{\gamma}_P\Omega_Y\Omega_Z\Omega_V}\right)\right] - \eta\bar{\gamma}_I\Omega_Z\left[\Omega_V\left(\bar{\eta}\bar{\gamma}_I\Omega_Y\Omega_U + \frac{\bar{\eta}\bar{\gamma}_I\Omega_U\tau}{\bar{\gamma}_P} + \frac{\eta\bar{\eta}\bar{\gamma}_I^2\Omega_Z}{\bar{\gamma}_P}\right)\right.\\
&\left.\left.\left.+ \frac{\bar{\eta}^2\bar{\gamma}_I^2\Omega_Y\Omega_U}{\bar{\gamma}_P}\right]\right.\\
&\times\exp\left(\frac{\bar{\eta}\bar{\gamma}_I\Omega_Y}{\bar{\gamma}_P\Omega_Z\Omega_V} + \frac{\eta\bar{\gamma}_I}{\bar{\gamma}_P\Omega_U} + \frac{\tau}{\bar{\gamma}_P\Omega_Y} + \frac{\tau}{\bar{\gamma}_P\Omega_Z}\right)\left[\mathrm{Ei}\left(\frac{\eta\bar{\gamma}_I\Omega_Z - \eta\bar{\gamma}_I\Omega_Y}{\bar{\gamma}_P\Omega_Y\Omega_U}\right) - \mathrm{Ei}\left(\frac{(\Omega_Z - \Omega_Y)(\eta\bar{\gamma}_I\Omega_Z + \Omega_U\tau)}{\bar{\gamma}_P\Omega_Y\Omega_Z\Omega_U}\right)\right]\Bigg\}\Bigg\} \qquad (12)
\end{aligned}
$$

some representative sample cases. Let us consider a two-dimensional topology, where the source, relay, and destination of the cognitive network and the destination of the primary network are located at $(0, 0)$, $(0.5, 0)$, $(1, 0)$, and $(0.25, 1)$, respectively. Additionally, with no loss of generality, let the average channel power of all wireless links be determined by the path-loss, i.e., $\Omega_A = d_A^{-\alpha}$, $A \in \{U, V, X, Y, Z\}$, where d_A is the distance between two terminals and α is the path-loss exponent. In our examples, the path-loss exponent and the target SNR threshold are set as $\alpha = 4$ and $\tau = 0$ dB, respectively. As for the average channel power of RSI, Ω_W, we have assumed a conservative position with respect to the self-interference mitigation at R, similarly to other related works on FD relaying (see,

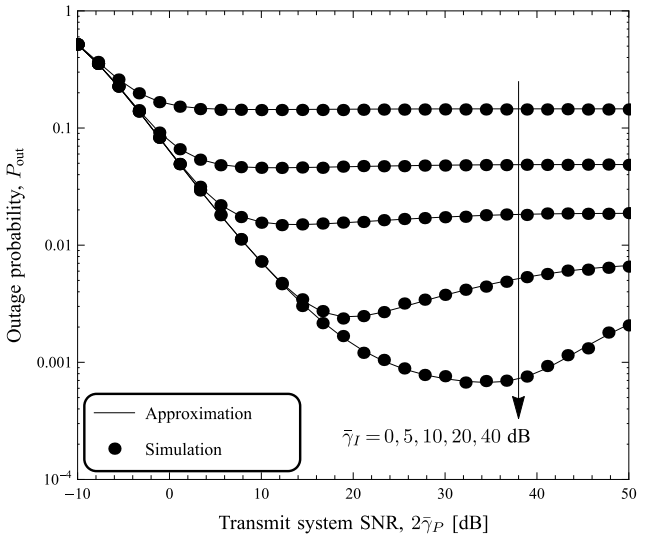

FIGURE 3. Outage performance against transmit system SNR, by considering distinct values of the interference power constraint $\bar{\gamma}_I$, for $\Omega_W = -20$ dB and $\eta = 0.5$.

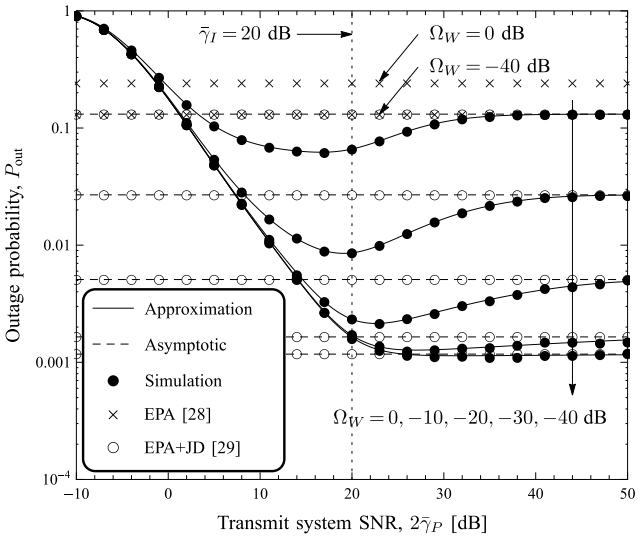

FIGURE 4. Outage performance against transmit system SNR, by considering distinct values of average channel power at the RSI link, Ω_W, for $\bar{\gamma}_I = 20$ dB and $\eta = 0.5$. For comparison, the exact outage probabilities for the schemes EPA [28, eq. (15)] and EPA+JD [29, eq. (8)] are also shown.

e.g., [18], [23], [28], [29]). By doing so, we aim to demonstrate that the system performance can be hampered by the self-interference. On the other hand, the RSI values assumed herein (−40 to 0 dB) are too high when compared to the recently claimed interference-cancellation (or attenuation) levels (70 to 100 dB) [13]–[15]. These experimental results show the potential and feasibility of FD communications, as some of those RSI levels are close to the noise floor. All in all, it is noteworthy that such interference-cancellation levels entail not only antenna isolation but also sophisticated active (analog and digital) cancellation techniques [16]. Thus, hardware limitations may diminish the performance gain of the FD operation mode.

The outage performance of the investigated network against the transmit SNR is shown in Fig. 3, for distinct values of the maximum interference constraint $\bar{\gamma}_I = 0$, 5, 10, 20, 40 dB, with $\Omega_W = -20$ dB and $\eta = 0.5$ (i.e., equal power allocation). We corroborate our analytical formulas via Monte Carlo simulations. As one can observe from Fig. 3, our approximation in (10) and the simulation results have an excellent match. Moreover, note that, as the primary destination relax the maximum interference constraint (increasing $\bar{\gamma}_I$), the performance of the secondary network improves, as expected. Also note that, for $\bar{\gamma}_I \geq 20$ dB, the system performance shows an increase in the outage probability at high SNR. This is explained by the fact that, differently from HD relaying schemes, the considered FD relaying scheme suffers from RSI. Thus, even though operating at high SNR, the outage performance worsens, since more transmit power is permitted to the relay, and, consequently, the deleterious effect of the RSI increases. This trade-off is further investigated next.

Fig. 4 shows the outage performance of the considered network for distinct values of average channel power at the RSI link, namely, $\Omega_W = 0, -10, -20, -30, -40$ dB. In this case, the maximum interference constraint and the power allocation factor are set as $\bar{\gamma}_I = 20$ dB and $\eta = 0.5$, respectively. For comparison, the outage probabilities of the schemes EPA [28, eq. (15)] and EPA+JD [29, eq. (8)] are also shown. For clarity, only the cases $\Omega_W = 0$ and −40 dB are shown for the EPA scheme. Again, note that the accuracy of our approximate and asymptotic expressions is corroborated by the simulation curves. Also note that, at the high-SNR regime, the system performance exhibits a floor, which is caused by two main factors: the RSI at the FD relay and the maximum interference power tolerated at the primary destination. For low RSI (e.g., $\Omega_W = -40$ dB), the outage probability is chiefly governed by the maximum interference constraint. Thus, the floor of the outage probability is observed to occur when the transmit system SNR approaches the interference constraint (i.e., $2\bar{\gamma}_P \approx \bar{\gamma}_I = 20$ dB). On the other hand, as the RSI increases, the outage floor level rises, thereby diminishing the outage performance, as expected. In particular, note that, as more transmit SNR is allowed, our scheme approaches the performance of the EPA+JD scheme, as expected. In addition, when a very low transmit SNR is allowed, our scheme is outperformed by the EPA+JD scheme (and even by the poorer EPA scheme). This is indeed quite intuitive, as the EPA and EPA+JD schemes have unbounded transmit SNRs. But less intuitive is the behavior at medium-to-high transmit SNR. In this range, the constrained transmit power in our scheme proves to be advantageous, leading to a lower outage probability. This is because the reduced transmit power is outbalanced by the corresponding reduced self-interference.

Fig. 5 shows the system throughput corresponding to the above-considered scenario, in which we have set $\bar{\gamma}_I = 20$ dB and $\eta = 0.5$, allowing for different values of average channel

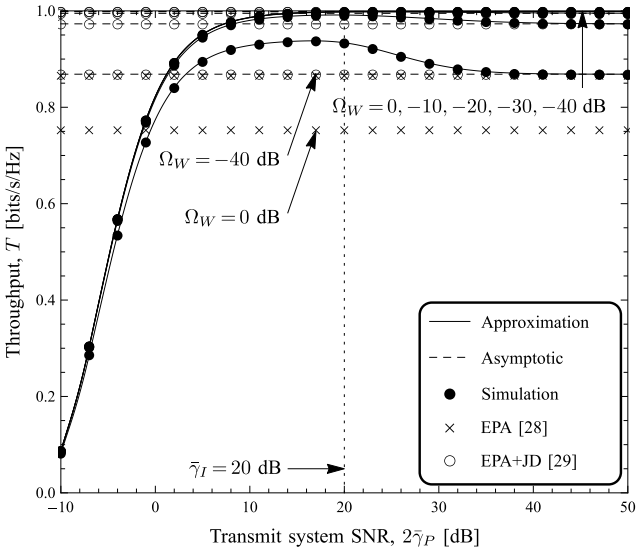

FIGURE 5. Throughput against transmit system SNR, by considering distinct values of average channel power at the RSI link, Ω_W, for $\bar{\gamma}_I = 20$ dB and $\eta = 0.5$. For comparison, the throughput for the schemes EPA [28, eq. (15)] and EPA+JD [29, eq. (8)] are also shown.

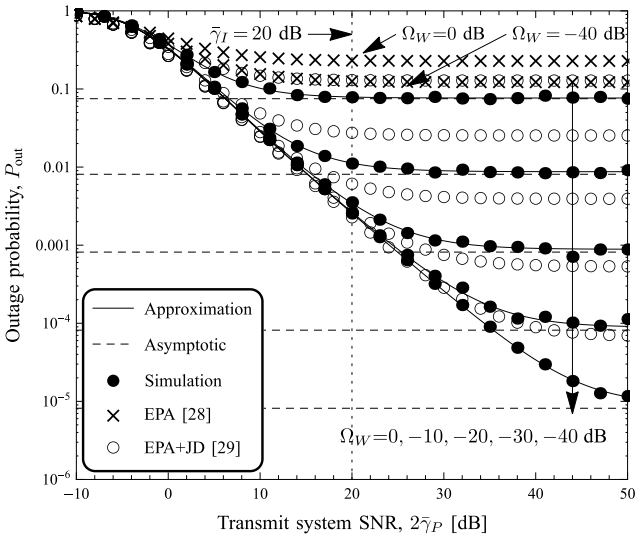

FIGURE 6. Outage performance against transmit system SNR, by considering distinct values of average channel power at the RSI link, Ω_W, for $P_T \propto I$ and $\eta = 0.5$. For comparison, the exact outage probabilities for the schemes EPA [28, eq. (15)] and EPA+JD [29, eq. (8)] are also shown.

power at the RSI link. Similarly to [23], herein the throughput is defined as the product of the spectral efficiency with the probability of successful transmissions, given in bits/s/Hz. Thus, by defining a target spectral efficiency $\mathcal{R}$, related to the target SNR threshold τ as $\mathcal{R} = \log_2(1 + \tau)$ for FD relaying, the system throughput is given by $T = \mathcal{R}(1 - P_{\text{out}})$. For illustration purposes, we have used $\mathcal{R} = 1$ or, equivalently, $\tau = 0$ dB. From the figure, we corroborate the fact that self-interference mitigation techniques play a key role in better exploiting the potentials of FD relaying, especially at medium-to-high SNR, as the lower is the RSI level, the higher is the achieved throughput. On the other hand, it is paramount to take into account the maximum-available transmit power at the secondary nodes, as it proves to limit the throughput performance achieved by EPA and EPA+JD schemes at low SNR, in which the secondary source and relay are allowed for unbounded transmit powers, defined as I/g_U and I/g_V, respectively [28], [29].

In Fig. 6, the outage performance of the system is assessed, for the same network setup considered in Fig. 4 (i.e., different values of Ω_W and η=0.5), except that, in this case, we consider $P_{\text{T}} \propto I$. Again, for comparison, the outage performance of EPA and EPA+JD schemes are presented. We can observe from Fig. 6 that the system performance also exhibits a floor, as expected. However, the key difference with respect to the performance shown in Fig. 4 (in which P_{T} varies independently of I) is that the outage saturation is only caused by the FD relaying operation, since as more transmit power is allowed at secondary terminals, the higher is the effect of RSI at the relay. In contrast, in Fig.4, the outage floor is governed by both the interference temperature I and RSI. Also note that the proposed scheme outperforms both EPA and EPA+JD schemes. This is due to the unbounded characteristic of the transmit power in EPA and EPA+JD schemes, such that poor channel conditions (or, equivalently, low channel gain values) of the interfering links $S \rightarrow P$ and $R \rightarrow P$ result in higher transmit powers at secondary terminals, thereby worsening the effect of RSI. Then, for such a condition of the interfering links, limiting the maximum-available transmit power shows to be beneficial to the system performance, as the effect of RSI is diminished.

In Fig. 7, the effect of the power allocation factor η between the terminals S and R on the outage probability is depicted. In this case, we have set $\bar{\gamma}_I = 20$ dB and $\Omega_W = -20$ dB.

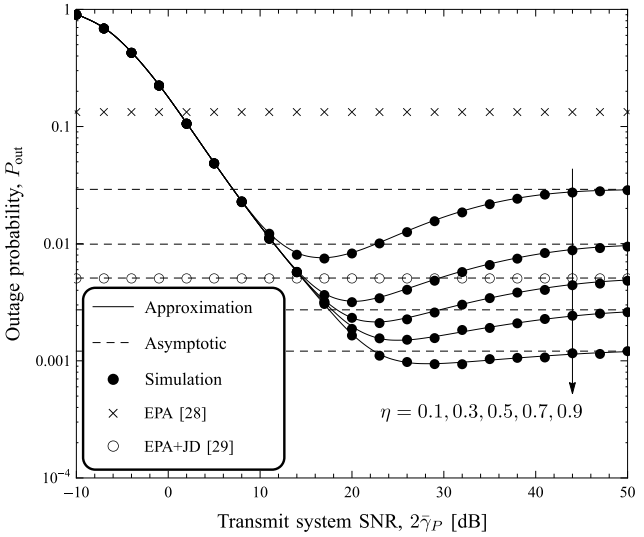

FIGURE 7. Outage probability against transmit system SNR, by considering distinct values of power allocation factor η, for $\bar{\gamma}_I = 20$ dB and $\Omega_W = -20$ dB.

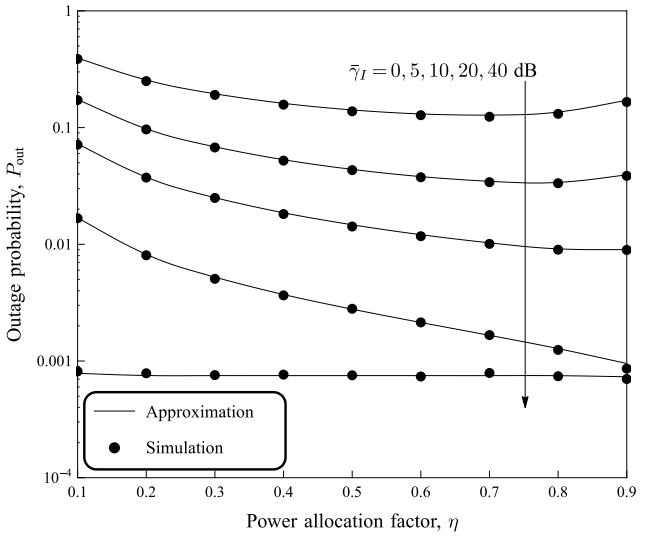

FIGURE 8. Outage probability against power allocation factor η, by considering distinct values of maximum interference constraint $\bar{\gamma}_I$, for $\Omega_W = -20$ dB and $2\bar{\gamma}_P = 30$ dB.

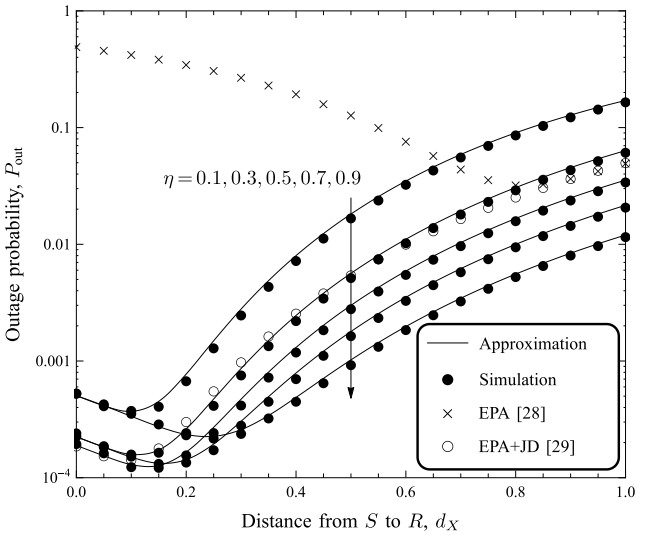

FIGURE 9. Outage probability against distance from source to relay, by considering distinct values of the power allocation factor η, for $\bar{\gamma}_I = 20$ dB, $\Omega_W = -20$ dB, and $2\bar{\gamma}_P = 30$ dB.

Note that the performance improves as more power is allocated to the source (increasing η). This is because the effect of the RSI diminishes, as less power is allocated to the relay. In particular, when $\eta > 0.5$, our scheme outperforms the EPA+JD scheme at medium-to-high SNR. On the other hand, one could infer from the behavior of the curves in Fig. 7 that the best strategy for communication would be to set $\eta = 1$ (or, equivalently, to dispense with R). However, it is worthwhile to point out that such a behavior resulted from the particular set of parameters considered in this specific example. This is not always true, as will be shown in the next figure.

Fig. 8 illustrates the outage probability against the power allocation factor η between the terminals S and R, by considering different values of the interference power constraint $\bar{\gamma}_I = 0, 5, 10, 20, 40$ dB, with $\Omega_W = -20$ dB and $2\bar{\gamma}_P = 30$ dB. As discussed above, in general, the outage performance improves as more power is allocated to the source (increasing η), and, consequently, less power is allocated to the relay, since we reduce the impact of the self-interference. However, for large $\bar{\gamma}_I$ (or, more specifically, for $\bar{\gamma}_I \geq 2\bar{\gamma}_P$), the secondary nodes transmit most frequently with maximum transmit power P_{T}, and thus varying η does not bring any additional gains. On the other hand, note that depending on the value of the maximum interference constraint $\bar{\gamma}_I$, a power allocation factor η different from 1 can be the optimal choice. For example, under stringent spectrum-sharing constraints (e.g., for $\bar{\gamma}_I = 0$ and 5 dB), the use of the secondary FD relay proves to be advantageous.

Fig. 9 shows the performance of the system under investigation in terms of the outage probability against the distance from S to R, d_X, by considering different values of the power allocation factor η. Here, the same two-dimensional topology of the previous examples is employed, except that the location of the secondary relay is varied along the distance between the secondary source and destination. Thus, the following relations hold: $0 < d_X < 1$ and $d_X + d_Y = 1$. In addition, to keep symmetry with respect to S and R, the location of the primary destination is set as $(d_X/2, 1)$. The other system parameters are set as $\bar{\gamma}_I = 20$ dB, $\Omega_W = -20$ dB, and $2\bar{\gamma}_P = 30$ dB. Also note in this case that, for $\eta > 0.5$, our scheme outperforms the EPA and EPA+JD schemes. Yet, when $\eta < 0.5$ and R is closer to D, our scheme deteriorates, being poorer than EPA.

V. CONCLUSIONS

This paper analyzed the outage probability for a cognitive network employing FD-DF transmission at the relay and JD reception at the destination, in an underlay spectrum-sharing scenario. We derived a tight approximate expression for the outage probability, obtained in closed form. Computer simulation results were provided to corroborate the high accuracy of our analytical approximation. The results showed that either the maximum interference power tolerated at the primary destination or the residual self-interference at the secondary relay may lead to an outage floor in the high SNR regime. This floor level was derived from an asymptotic outage analysis and expressed as a function of key system parameters.

APPENDIX A
PROOF OF LEMMA 1

Here, analytical expressions for the CDF and PDF of X are provided in closed form. From (2) and (4a), the CDF of X can be determined as

$$\begin{aligned} F_X(x) &= \Pr\left[\min\left\{\frac{\eta\bar{\gamma}_I}{g_U}, \bar{\gamma}_P\right\} g_X < x\right] \\ &= \Pr\left[g_X\bar{\gamma}_P < x, g_U \leq \frac{\eta I}{P_{\mathrm{T}}}\right] \\ &\quad + \Pr\left[g_X\eta\bar{\gamma}_I < g_U x, g_U > \frac{\eta I}{P_{\mathrm{T}}}\right] \end{aligned}$$

$$\overset{(a)}{=} F_{g_X}\left(\frac{x}{\bar{\gamma}_P}\right) F_{g_U}\left(\frac{\eta\bar{\gamma}_I}{\bar{\gamma}_P}\right) + \int_{\frac{\eta\bar{\gamma}_I}{\bar{\gamma}_P}}^{\infty} F_{g_X}\left(\frac{ux}{\eta\bar{\gamma}_I}\right) f_{g_U}(u)\, du$$

$$\overset{(b)}{=} \left(1 - e^{-\frac{x}{\bar{\gamma}_P\Omega_X}}\right)\left(1 - e^{-\frac{\eta\bar{\gamma}_I}{\bar{\gamma}_P\Omega_U}}\right) + e^{-\frac{\eta\bar{\gamma}_I}{\bar{\gamma}_P\Omega_U}} - \frac{\eta\bar{\gamma}_I\Omega_X e^{-\frac{\eta\bar{\gamma}_I}{\bar{\gamma}_P}\left(\frac{1}{\Omega_U}+\frac{x}{\eta\bar{\gamma}_I\Omega_X}\right)}}{\eta\bar{\gamma}_I\Omega_X + \Omega_U x}, \quad (15)$$

where in step (a) we have used that $I/P_{\mathrm{T}} = \bar{\gamma}_I/\bar{\gamma}_P$, and step (b) follows since g_X and g_U are exponentially distributed variates with average values given respectively by Ω_X and Ω_U. Then, by some mathematical manipulations, an useful analytical expression for the CDF of X is attained in closed form as in (8). Moreover, by employing [42, eq. (4.13)], the PDF of X can be obtained from (8) as

$$f_X(x) = \frac{d}{dx} F_X(x), \quad (16)$$

from which, by some mathematical manipulations, a closed-form expression for the PDF of X is attained as in (9), thus concluding the proof.

APPENDIX B
PROOF OF THEOREM 1

Here, a highly approximate solution for the outage probability of underlay cognitive FD-DF relaying networks employing JD reception at the secondary destination is obtained in closed form. As aforementioned, finding the joint CDF $F_{\gamma_R,\gamma_D}(\cdot,\cdot)$ in (7) proves to be extremely intricate. On the other hand, we have empirically verified through exhaustive simulations that an analysis performed under the assumption of independence between γ_R and γ_D, so that $F_{\gamma_R,\gamma_D}(\cdot,\cdot) = F_{\gamma_R}(\cdot)F_{\gamma_D}(\cdot)$, renders an excellent approximate solution to the exact outage performance of the considered scheme, as can be seen by illustrative examples in Section IV.[2] Therefore, the outage probability in (7) can be well approximated by (10). Note in the latter expression that, differently from (7), only the marginal CDFs of γ_R and γ_D are needed to completely determine P_{out}. From (5) and (6), the CDFs of γ_R and γ_D can be obtained as

$$F_{\gamma_R}(\tau) = \Pr\left[\frac{X}{1+W} < \tau\right] = \int_0^{\infty} F_X(\tau(1+w)) f_W(w)\, dw, \quad (17)$$

$$F_{\gamma_D}(\tau) = \Pr[Y + Z < \tau] = \int_0^{\tau} F_Z(\tau - y) f_Y(y)\, dy. \quad (18)$$

In light of (17) and (18), the CDFs of X and Z, as well as the PDFs of W and Y, are required in order to compute the outage probability in (10). Then, by invoking Lemma 1 and substituting the corresponding probability functions into (17) and (18), after lengthy simplifications, (11) and (12) are obtained. Finally, by plugging the latter expressions into (10), we obtain a new accurate approximation, given in closed form, for the outage probability of underlay CRNs operating under FD-DF relaying and JD reception at the secondary destination, which concludes the proof.

[2] As mentioned before, such an assumption was also exploited in previous related works (e.g. [28], [29], [32]).

REFERENCES

[1] Nokia Solutions and Networks, "Looking ahead to 5G," White Paper, 2014.

[2] Ericsson, "5G radio access: Technology and capabilities," White Paper, Feb. 2015.

[3] J. G. Andrews *et al.*, "What will 5G be?" *IEEE J. Sel. Areas Commun.*, vol. 32, no. 6, pp. 1065–1082, Jun. 2014.

[4] X. Hong, J. Wang, C.-X. Wang, and J. Shi, "Cognitive radio in 5G: A perspective on energy-spectral efficiency trade-off," *IEEE Commun. Mag.*, vol. 52, no. 7, pp. 46–53, Jul. 2014.

[5] Z. Zhang, X. Chai, K. Long, A. V. Vasilakos, and L. Hanzo, "Full duplex techniques for 5G networks: Self-interference cancellation, protocol design, and relay selection," *IEEE Commun. Mag.*, vol. 53, no. 5, pp. 128–137, May 2015.

[6] J. Mitola and G. Q. Maguire, Jr., "Cognitive radio: Making software radios more personal," *IEEE Pers. Commun.*, vol. 6, no. 4, pp. 13–18, Apr. 1999.

[7] S. Srinivasa and S. Ali Jafar, "The throughput potential of cognitive radio: A theoretical perspective," *IEEE Commun. Mag.*, vol. 45, no. 5, pp. 73–79, May 2007.

[8] A. Goldsmith, S. A. Jafar, I. Maric, and S. Srinivasa, "Breaking spectrum gridlock with cognitive radios: An information theoretic perspective," *Proc. IEEE*, vol. 97, no. 5, pp. 894–914, Apr. 2009.

[9] S. Haykin, "Cognitive radio: Brain-empowered wireless communications," *IEEE J. Sel. Areas Commun.*, vol. 23, no. 2, pp. 201–220, Feb. 2005.

[10] A. Sendonaris, E. Erkip, and B. Aazhang, "User cooperation diversity. Part I. System description," *IEEE Trans. Commun.*, vol. 51, no. 11, pp. 1927–1948, Nov. 2003.

[11] J. N. Laneman, D. N. C. Tse, and G. W. Wornell, "Cooperative diversity in wireless networks: Efficient protocols and outage behavior," *IEEE Trans. Inf. Theory*, vol. 50, no. 12, pp. 3062–3080, Dec. 2004.

[12] F. Gomez-Cuba, R. Asorey-Cacheda, and F. J. Gonzalez-Castano, "A survey on cooperative diversity for wireless networks," *IEEE Commun. Surveys Tuts.*, vol. 14, no. 3, pp. 822–835, 3rd Quart., 2012.

[13] M. Duarte, C. Dick, and A. Sabharwal, "Experiment-driven characterization of full-duplex wireless systems," *IEEE Trans. Wireless Commun.*, vol. 11, no. 12, pp. 4296–4307, Dec. 2012.

[14] S. Hong *et al.*, "Applications of self-interference cancellation in 5G and beyond," *IEEE Commun. Mag.*, vol. 52, no. 2, pp. 114–121, Feb. 2014.

[15] A. Sabharwal, P. Schniter, D. Guo, D. W. Bliss, S. Rangarajan, and R. Wichman, "In-band full-duplex wireless: Challenges and opportunities," *IEEE J. Sel. Areas Commun.*, vol. 32, no. 9, pp. 1637–1652, Sep. 2014.

[16] B. Debaillie *et al.*, "Analog/RF solutions enabling compact full-duplex radios," *IEEE J. Sel. Areas Commun.*, vol. 32, no. 9, pp. 1662–1673, Sep. 2014.

[17] T. Riihonen, S. Werner, and R. Wichman, "Mitigation of loopback self-interference in full-duplex MIMO relays," *IEEE Trans. Signal Process.*, vol. 59, no. 12, pp. 5983–5993, Dec. 2011.

[18] T. Riihonen, S. Werner, and R. Wichman, "Hybrid full-duplex/half-duplex relaying with transmit power adaptation," *IEEE Trans. Wireless Commun.*, vol. 10, no. 9, pp. 3074–3085, Sep. 2011.

[19] H. Alves, D. B. da Costa, R. D. Souza, and M. Latva-aho, "Performance of block-Markov full duplex relaying with self interference in Nakagami-*m* fading," *IEEE Wireless Commun. Lett.*, vol. 2, no. 3, pp. 311–314, Jun. 2013.

[20] H. Alves, "On the performance analysis of full-duplex networks," Ph.D. dissertation, Dept. Elect. Eng., Univ. Oulu, Oulu, Finland, 2015.

[21] M. Khafagy, A. Ismail, M.-S. Alouini, and S. Aissa, "Efficient cooperative protocols for full-duplex relaying over Nakagami-*m* fading channels," *IEEE Trans. Wireless Commun.*, vol. 14, no. 6, pp. 3456–3470, Jun. 2015.
[22] Y. Wang, Y. Xu, N. Li, W. Xie, K. Xu, and X. Xia, "Relay selection of full-duplex decode-and-forward relaying over Nakagami-*m* fading channels," *IET Commun.*, vol. 10, no. 2, pp. 170–179, Jan. 2016.
[23] D. P. M. Osorio, E. E. B. Olivo, H. Alves, J. C. S. S. Filho, and M. Latva-aho, "Exploiting the direct link in full-duplex amplify-and-forward relaying networks," *IEEE Signal Process. Lett.*, vol. 22, no. 10, pp. 1766–1770, Oct. 2015.
[24] E. E. B. Olivo, D. P. M. Osorio, D. B. D. Costa, and J. C. S. S. Filho, "Multiuser incremental decode-and-forward relaying under outdated channel estimates," *Electron. Lett.*, vol. 51, no. 4, pp. 369–371, Feb. 2015.
[25] A. Carleial, "Multiple-access channels with different generalized feedback signals," *IEEE Trans. Inf. Theory*, vol. IT-28, no. 6, pp. 841–850, Nov. 1982.
[26] F. M. J. Willems, "Informationtheoretical results for the discrete memoryless multiple access channel," Ph.D. dissertation, Katholieke Univ. Leuven, Leuven, Belgium, Oct. 1982.
[27] G. Kramer, M. Gastpar, and P. Gupta, "Cooperative strategies and capacity theorems for relay networks," *IEEE Trans. Inf. Theory*, vol. 51, no. 9, pp. 3037–3063, Sep. 2005.
[28] H. Kim, S. Lim, H. Wang, and D. Hong, "Optimal power allocation and outage analysis for cognitive full duplex relay systems," *IEEE Trans. Wireless Commun.*, vol. 11, no. 10, pp. 3754–3765, Oct. 2012.
[29] S. Mafra, H. Alves, D. B. Da Costa, R. D. Souza, E. M. G. Fernandez, and M. Latva-aho, "On the performance of cognitive full-duplex relaying under spectrum sharing constraints," *EURASIP J. Wireless Commun. Netw.*, vol. 2015, no. 1, p. 169, Jun. 2015.
[30] M. Khafagy, M.-S. Alouini, and S. Aissa, "Full-duplex opportunistic relay selection in future spectrum-sharing networks," in *Proc. IEEE Int. Conf. Commun. Workshop (ICCW)*, London, U.K., Jun. 2015, pp. 1196–1200.
[31] B. Zhong, Z. Zhang, X. Chai, Z. Pan, K. Long, and H. Cao, "Performance analysis for opportunistic full-duplex relay selection in underlay cognitive networks," *IEEE Trans. Veh. Technol.*, vol. 64, no. 10, pp. 4905–4910, Oct. 2015.
[32] Y. Deng, K. Kim, T. Duong, M. Elkashlan, G. Karagiannidis, and A. Nallanathan, "Full-duplex spectrum sharing in cooperative single carrier systems," in *Proc. IEEE WCNC*, New Orleans, LA, USA, Mar. 2015, pp. 25–30.
[33] Y. Deng, K. J. Kim, T. Q. Duong, M. Elkashlan, G. K. Karagiannidis, and A. Nallanathan, "Full-duplex spectrum sharing in cooperative single carrier systems," *IEEE Trans. Cognit. Commun. Netw.*, vol. 2, no. 1, pp. 68–82, Mar. 2016.
[34] B. Zhong and Z. Zhang, "Opportunistic two-way full-duplex relay selection in underlay cognitive networks," *IEEE Syst. J.*, vol. 12, no. 1, pp. 725–734, Mar. 2016.
[35] E. E. B. Olivo, D. P. M. Osorio, H. Alves, J. C. S. S. Filho, and M. Latva-aho, "An adaptive transmission scheme for cognitive decode-and-forward relaying networks: Half duplex, full duplex, or no cooperation," *IEEE Trans. Wireless Commun.*, vol. 15, no. 8, pp. 5586–5602, Aug. 2016.
[36] N.-P. Nguyen, C. Kundu, H. Q. Ngo, T. Q. Duong, and B. Canberk, "Secure full-duplex small-cell networks in a spectrum sharing environment," *IEEE Access*, vol. 4, pp. 3087–3099, 2016.
[37] X.-T. Doan, N.-P. Nguyen, C. Yin, D. B. da Costa, and T. Q. Duong, "Cognitive full-duplex relay networks under the peak interference power constraint of multiple primary users," *EURASIP J. Wireless Commun. Netw.*, vol. 2017, no. 1, p. 8, Jan. 2017.
[38] T. M. C. Chu and H.-J. Zepernick, "On capacity of full-duplex cognitive cooperative radio networks with optimal power allocation," in *Proc. IEEE WCNC*, San Francisco, CA, USA, Mar. 2017, pp. 1–6.
[39] T. M. Cover and A. A. El Gamal, "Capacity theorems for the relay channel," *IEEE Trans. Inf. Theory*, vol. IT-25, no. 5, pp. 572–584, Sep. 1979.
[40] I. S. Gradshteyn and I. M. Ryzhik, *Table of Integrals, Series and Products*, 7th ed. New York, NY, USA: Academic, 2007.
[41] L. Zheng and D. N. C. Tse, "Diversity and multiplexing: A fundamental tradeoff in multiple-antenna channels," *IEEE Trans. Inf. Theory*, vol. 49, no. 5, pp. 1073–1096, May 2003.
[42] A. Papoulis, *Probability, Random Variables, and Stochastic Processes*, 4th ed. New York, NY, USA: McGraw-Hill, 2002.

EDGAR EDUARDO BENITEZ OLIVO (M'16) received the B.Sc. degree in electronics and telecommunications engineering from the Armed Forces University-ESPE, Sangolquí, Ecuador, in 2008, and the M.Sc. and Ph.D. degrees in electrical engineering from the University of Campinas, Campinas, Brazil, in 2011 and 2015, respectively. In 2014, he held a visiting researcher position with the Centre for Wireless Communications, University of Oulu, Finland. He is currently an Assistant Professor with São Paulo State University, Campus of São Jõao da Boa Vista, Brazil. His research interests include the area of wireless communications, with a current focus on emerging technologies towards 5G wireless networks. He has served as a reviewer and TPC member for many journals and conferences.

DIANA PAMELA MOYA OSORIO (M'16) was born in Quito, Ecuador. She received the B.Sc. degree in electronics and telecommunications engineering from the Armed Forces University-ESPE, Sangolquí, Ecuador, in 2008, and the M.Sc. and D.Sc. degrees in electrical engineering from the University of Campinas, Campinas, Brazil, in 2011 and 2015, respectively. She is currently an Assistant Professor with the Department of Electrical Engineering, Federal University of São Carlos, São Carlos, Brazil. Her research interests include wireless communications in general, cooperative relaying networks, cognitive radio systems, PHY security, and 5G networks.

HIRLEY ALVES (S'11–M'16) received the B.Sc. degree in electrical engineering and the M.Sc. degree in electrical engineering from the Federal University of Technology-Paraná (UTFPR), Brazil, in 2010 and 2011, respectively, and the dual D.Sc. degree from the University of Oulu and UTFPR in 2015. He has been an Adjunct Professor of machine-type wireless communications, Centre for Wireless Communications, University of Oulu, Oulu, Finland, since 2017. He is actively involved in massive connectivity and ultra-reliable low latency communications. His research interests include wireless and cooperative communications, wireless full-duplex communications, PHY-security, and ultra-reliable communications mechanisms for future machine type wireless networks. He is a co-recipient of the 2017 IEEE International Symposium on Wireless Communications and Systems Best Student Paper Award, and a co-recipient of the 2016 Research Award from the Cuban Academy of Sciences. He has acted as an organizer, chair, and serves as a TPC and tutorial lecturer to several renowned international conferences.

JOSÉ CÂNDIDO SILVEIRA SANTOS FILHO (M'09) received the B.Sc., M.Sc., and Ph.D. degrees from the School of Electrical and Computer Engineering (FEEC), University of Campinas (UNICAMP), Campinas, Brazil, in 2001, 2003, and 2006, respectively, all in electrical engineering.. From 2006 to 2009, he was a Post-Doctoral Fellow with the Wireless Technology Laboratory, FEEC-UNICAMP. He is currently an Assistant Professor with FEEC-UNICAMP. Since 2011, he has been a Consultant for Bradar Indústria S.A., a branch of Embraer Defense and Security, in the development of innovative radar techniques. He has authored over 80 technical papers, about half of which are in international journals, and has served as a reviewer for many journals and conferences. His research interests include wireless communications and radar systems. He was ranked first in his undergraduate program, and his Ph.D. thesis received an Honorary Mention from the Brazilian Ministry of Education (CAPES) in the 2007 CAPES Thesis Contest.

MATTI LATVA-AHO (S'96–M'98–SM'06) was born in Kuivaniemi, Finland, in 1968. He received the M.Sc., Lic.Tech., and Dr. Tech. (Hons.) degrees in electrical engineering from the University of Oulu, Finland, in 1992, 1996, and 1998, respectively. From 1992 to 1993, he was a Research Engineer with Nokia Mobile Phones, Oulu, Finland. From 1994 to 1998, he was a Research Scientist with the Telecommunication Laboratory and Centre for Wireless Communications, University of Oulu. He was the Director of the Centre for Wireless Communications, University of Oulu, from 1998 to 2006. He is currently the Department Chair Professor of Digital Transmission Techniques and the Head of the Department of Communications Engineering, University of Oulu. He is the Head of the Centre for Wireless Communications and leads the activities related to 5G and 5G test networks. He has published over 200 conference or journal papers in the field of wireless communications. His research interests are related to mobile broadband wireless communication systems. He has been the TPC Chairman for PIMRC06, the TPC Co-Chairman for ChinaCom07, and the General Chairman for WPMC08.